Computational Investigation of Neutron Field modified with Various Materials

Alvie A. Astronomo[1], Eric M. Inocencio[4*], Cheri Anne M. Dingle[2], Frederick C. Hila[2], Kristine D. Romallosa[3] and Roland C. Caballar[5]
[1]Nuclear Reactor Operations Section
[2]Applied Physics Research Section
[3]Radiation Protection Services Section
Department of Science and Technology – Philippine Nuclear Research Institute (DOST-PNRI), Quezon City, 1100 Philippines

[4]Graduate School
University of Santo Tomas
Sampaloc, Manila 1008 Philippines
[*]*eric.inocencio.gs@ust.edu.ph*

[5]Quirino Memorial Medical Center
Quezon City, 1101 Philippines

Date received: June 2, 2021
Revision accepted: August 25, 2021

Abstract

Medical accelerators, such as cyclotrons for Positron Emission Tomography (PET) and linear accelerators (LINAC), generate neutrons as a byproduct during operation. Neutron fields in these facilities tend to vary depending on the facility design as well as the presence of various materials in the facility. Unfortunately, these variations in the neutron field cannot be accounted for by neutron survey meters that are typically deployed in the workplace for radiation monitoring. In this work, the researchers used Monte-Carlo-N-Particle (MCNP) 6.1 to investigate the extent of field modification with materials that are commonly found in accelerator facilities. A computational investigation was performed using the field of the ^{252}Cf source in the Philippine Nuclear Research Institute Neutron Laboratory (PNL) that was modified using polyethylene, lead, concrete and water. Variations in the spatial and energy distribution of neutron fluence as a result of introducing each modifier were presented. It was found that the relative deviation in the neutron dose due to polyethylene, lead, concrete and water modifiers were 96, 47, 83 and 94%, respectively. The result of this work was used as a basis for experiments performed at the PNL to investigate the limitations of commercial neutron survey meters when conducting dose measurements in different neutron fields.

***Keywords**:* MCNP, neutron field modification, neutron spectrum, neutron transport

1. Introduction

Neutrons have inherent properties that allow them to have wide-ranging applications in various disciplines. Currently, the major neutron sources in the

Philippine setting are medical accelerators where neutrons are produced as a byproduct when accelerated charged particles with sufficient energy hit heavy targets. These medical accelerators include cyclotrons for Positron Emission Tomography (PET) and linear accelerator (LINAC) facilities. Neutron field characterization is essential to evaluate the potential neutron dose to radiation workers, LINAC patients and the public for these applications.

The neutron dose is strongly dependent on the characteristic of the neutron field. However, it is only recently that neutron field characterization was performed in local medical accelerator facilities (Fontanilla *et al*., 2020; Solmeron *et al*., 2020). To date, only one PET cyclotron facility and one linear accelerator facility have neutron field data in the Philippines. However, neutron fields tend to vary depending on facility design, which includes the facility dimensions, the materials available in the facility that are used for shielding and the composition of materials in the facility. Each medical accelerator facility that operates under certain conditions will have a unique neutron field, thus warranting the importance of neutron field characterization, at least once, for a medical accelerator facility with neutron byproducts.

In this work, the researchers investigated the effect of different materials on the neutron field that is produced by a ^{252}Cf source in the Philippine Nuclear Research Institute Neutron Laboratory (PNL) to demonstrate the significance of neutron field characterization for facilities with varying configurations. The ^{252}Cf source was used in this study as it is one of the most commonly employed radioisotopes for calibrating neutron survey meters deployed in a medical cyclotron and LINAC facilities. Although the neutron spectra of the sources are different – with accelerators-generated neutrons having an evaporation reaction spectrum and the ^{252}Cf neutrons with spontaneous fission spectrum – the modification of the ^{252}Cf spectrum can simulate the spectra in medical accelerators at certain locations. Furthermore, information about the source neutron spectrum was eventually modified due to multiple interactions with the materials in the facility (Fontanilla *et al*., 2020), thus further supporting the motivation of this study.

2. Methodology

A detailed MCNP model of the ^{252}Cf source in the PNL irradiation room was prepared based on manufacturer specifications and facility drawings (Grande *et al*., 2020). The ^{252}Cf spectrum based on ENDF VII.1 (Chadwick *et al*.,

2011) was used for the source term and declared as a point source, with a strength of 1.11 x 10^7 n/s (Hila *et al*., 2021). Material compositions in the model, which are summarized in Table 1, were obtained from the PNL compendium of materials (McConn *et al*., 2011).

Table 1. Material composition and densities used in the MCNP model (McConn *et al*., 2011)

Material	Item	Density (g/cm^3)	Composition* (Atom fraction)
Air	Air, detector sphere	0.001205	C (0.000150); N (0.784431); O (0.210748); Ar (0.004671);
Regular concrete	Wall, floor, ceiling, concrete modifier	2.300000	H (0.168038); O (0.563183); Na (0.021365); Al (0.021343; ^{28}Si (0.187425); ^{29}Si (0.009521); ^{30}Si (0.006284); ^{40}Ca (0.018025); ^{42}Ca (0.0001203); ^{43}Ca (0.000025); ^{44}Ca (0.000388); ^{46}Ca (0.00000074); ^{48}Ca (0.000035); ^{54}Fe (0.000248); ^{56}Fe (0.003896); ^{57}Fe (0.000089); ^{58}Fe (0.00001197)
Stainless steel 304 L	Source encapsulation	8.00295	C (0.000687); ^{28}Si (0.009031); ^{29}Si (0.000459); ^{30}Si (0.000303); ^{31}P (0.000408); ^{32}S (0.000244); ^{33}S (0.000002); ^{34}S (0.000011); ^{50}Cr (0.008734); ^{52}Cr (0.168429); ^{53}Cr (0.019098); ^{54}Cr (0.004754); ^{55}Mn (0.010013); ^{54}Fe (0.039986); ^{56}Fe (0.627690); ^{57}Fe (0.014496); ^{58}Fe (0.001929); ^{58}Ni (0.063805); ^{60}Ni (0.024578); ^{61}Ni (0.001068); ^{62}Ni (0.003407); ^{64}Ni (0.000867)
Carbon steel	Detector platform	0.41667**	C (0.022831); ^{54}Fe (0.057115); ^{56}Fe (0.896591); ^{57}Fe (0.020706); ^{58}Fe (0.002755)
Water	Water modifier (water, liquid)	0.998207	H (0.666657), O (0.333343)
Lead	Lead modifier	6.220000	O (0.592955), Si (0.174592), Ti (0.010251), As (0.002146), Pb (0.220056)
Polyethylene	Polyethylene modifier	1.000000	H (0.627759), B (0.046690), C (0.325552)

* Those with no mass numbers were declared according to their natural abundance; **density value was corrected to address the irregular shape of the detector platform.

Figure 1 shows the simulation model used in this investigation, which included the concrete walls and floors as well as the air in the bound volume

of the walls. Additional details for the modeling of the PNL irradiation room were described in previously published works (Asuncion-Astronomo *et al*., 2020, 2021). To minimize computational time, mesh calculations were limited in the area bound by the red dashed lines in Figure 1, which is then magnified in Figure 2. The detector holder material was declared as air to emphasize the modifier's effect on the neutron field. The carbon steel detector platform was modeled as a carbon steel block with density correction to account for the irregular shape of the platform design.

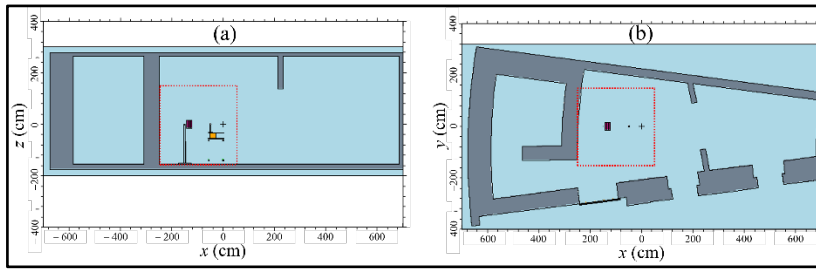

Figure 1. MCNP model of the irradiation set up that is investigated in x-z (a) and x-y (b) planes

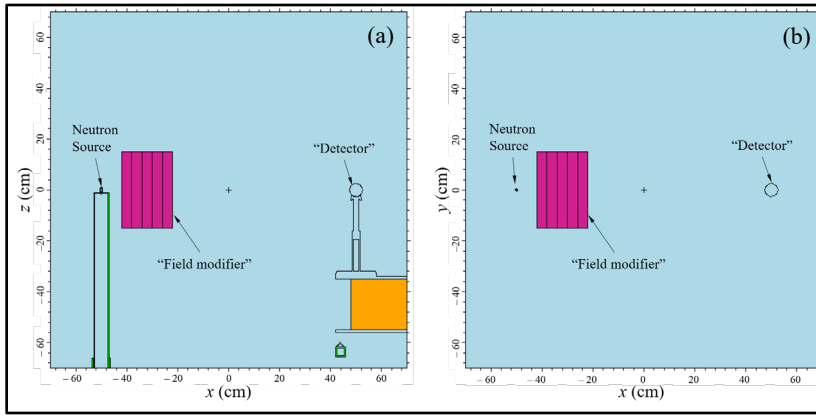

Figure 2. Magnified MCNP model of the irradiation set up that is investigated in x-z (a) and x-y (b) planes

The field modifier (FM) was declared as five adjacent slab cells, such that the total dimension of the FM is 20 x 30 x 30 cm cells. The center face of the FM was positioned at a 1.5-m distance from the floor with the same level and at a 5-cm distance from the source (Figure 2) as per the International Organization for Standardization (ISO) 8529-2: 2000 standards (ISO, 2000). The material declared in the FM cells was varied to investigate the effect of different

materials on the PNL neutron field. Materials considered for this investigation were polyethylene, lead, concrete and water, which are commonly found in medical accelerator facilities as radiation shielding and main components of the building design. While concrete and lead are typical shielding materials, polyethylene and water are known moderators of neutrons, which can be used for machine calibration for radiation dosimetry and radiation protection. The use of water phantoms is a golden standard for calibrating LINAC machines for they are well-known as tissue-equivalent materials (Vega-Carillo *et al*., 2010; Cevallos-Robalino *et al*., 2019; Qi *et al*., 2021).

A 5-cm air-sphere cell located at 1 m from the source was used to serve as the detector for this investigation. To determine the total neutron fluence rate and the neutron spectrum at the detector cell, the F4 tally of MCNP was employed. The spectrum was calculated for the neutron energy range from 1 to 100 MeV divided into 120 equidistant logarithmic intervals. This energy range was chosen to correspond with that of the calculated response function of the He-based spectrometer, which was for the experimental validation of the computational results.

Meanwhile, the FMESH tally of MCNP was used to calculate the horizontal and vertical spatial distribution of neutrons in 300 x 300 x 20 cm meshes, with mesh element volume of 0.125 cm^3, which were centered at 50 cm from the source. The vertical and horizontal meshes superimposed in the computational model of the PNL irradiation room are illustrated in Figure 3.

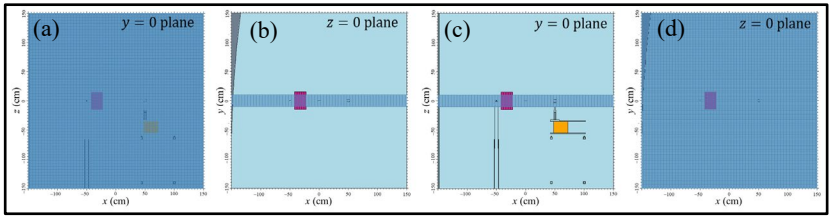

Figure 3. Vertical mesh with dimensions of 300 x 20 x 300 cm (a-b), and horizontal mesh with dimensions of 300 x 300 x 20 cm (c-d) superimposed in the computational model to determine the neutron fluence rate distribution

The simulated neutron fields obtained with different modifier materials were then compared with the neutron field when the cell material was declared as air. All calculations were performed using the most recent cross-section data library available ENDF/B VIII.0 (Brown *et al*., 2018), and thermal neutron scattering data S(α,β) – poly.10t and lwtr.10t for polyethylene and water, respectively. The poly.10t data was also used to estimate thermal neutron

scattering for concrete. The variance reduction technique used was the Russian roulette biasing with an importance ratio = 2 in the 5-cm shell. A total of 1 x 109 particles were used in the simulations to attain uncertainties below 0.5% for the results.

3. Results and Discussion

3.1 Variation in Total Neutron Fluence Rate and Neutron Spectra

Figure 4 presents a comparison of neutron fluence rate values that were calculated at the detector location for fields with different field modifiers. As expected, a significant reduction in the fluence rate was observed when modifiers were present in the calculation setup, which demonstrates that the spectrum modifiers also have a shielding effect as it is located between the source and the detector. Nevertheless, the simple calculation of the total fluence rate did not provide information on how the spectrum has been modified. For this purpose, the energy distribution of neutrons was also determined as described in section 2.

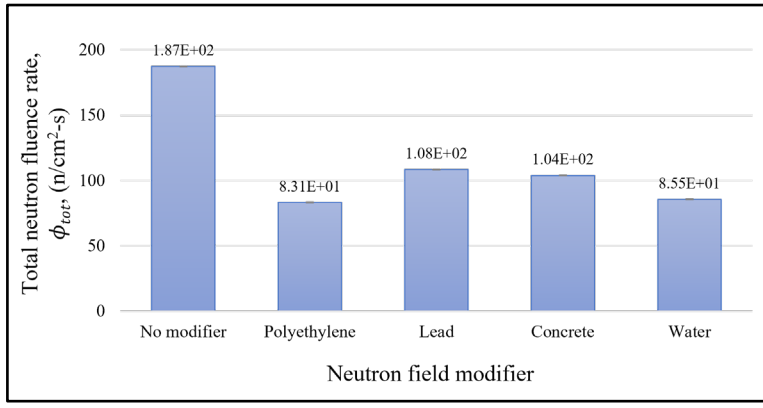

Figure 4. Total neutron fluence rate at the detector location for different field modifiers; uncertainties are less than 0.5%.

The calculated unit neutron spectra for all modifiers and the spectra normalized per total fluence are presented in Figure 5. Two representations of the spectra were provided to emphasize distinct features of the neutron energy distribution. The unit spectra (Figure 5a), which is the number of neutrons per energy bin per unit fluence rate, provides a clear image of the differences in the spectrum in the thermal (E < 0.625 eV) and epithermal (E = 0.625 eV to

0.1 MeV) neutron energy range. Meanwhile, the normalized spectra in Figure 5b were obtained by normalizing the unit spectra to the total fluence rate per modifier. The latter representation gives a useful comparison of the modifier effects on the spectrum. The overlapping plots of the water- and PE-modified spectra in Figure 5b are readily observed, which was due to the similar neutron moderation mechanisms in these materials. The observed differences in the spectrum plots were further elaborated in the data presented in Table 2 and Table 3.

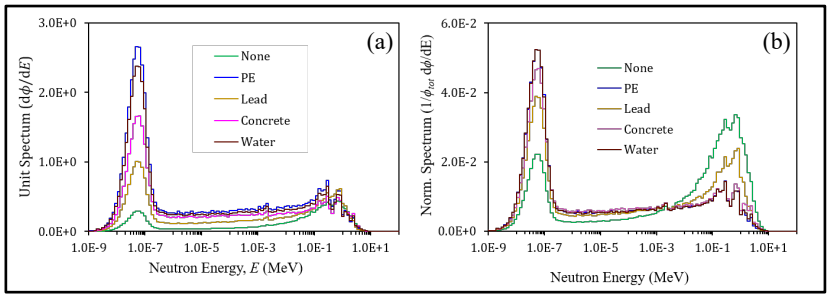

Figure 5. Unit neutron spectra at the detector location for different field modifiers (a) and normalized spectrum at the detector location for different field modifiers (b)

The components of neutrons in terms of energy range that was calculated for different modifiers are provided in Tables 2 and 3. Table 2 presents the component breakdown of the total neutron fluence rate that is given in Figure 4.

Table 2. Neutron components in terms of energy range

Field modifier	Neutron fluence rate, ϕ (n/cm^2-s)			
	Thermal (E < 0.625 eV)	Epithermal (0.625 eV ≤ E ≥ 0.1 MeV)	Fast (E > 0.1 MeV)	Total
None	5.97E+01	4.44E+01	8.21E+01	1.87E+02
PE	5.68E+01	1.40E+01	1.17E+01	8.31E+01
Lead	5.83E+01	2.09E+01	2.84E+01	1.08E+02
Concrete	6.77E+01	1.84E+01	1.70E+01	1.04E+02
Water	5.83E+01	1.43E+01	1.24E+01	8.55E+01

Table 3 presents the data in percentage with neutron components of the ^{252}Cf spectrum included for comparison. As shown in Table 3, the ^{252}Cf neutron source emitted predominantly fast neutrons (70.68%), but at the detector location, the fast neutron component was significantly reduced at 43.81%

while the thermal component was higher (31.86%). This was due to neutrons scattered by the concrete wall and the detector stand that was also declared in the computational model, which demonstrates how a facility design can modify the field.

Table 3. Percent distribution of neutron components in terms of energy range

Field modifier	Percentage of neutron fluence rate (%)		
	Thermal (E < 0.625 eV)	Epithermal (0.625 eV ≤ E ≥ 0.1 MeV)	Fast (E > 0.1 MeV)
$^{252}Cf^{*}$	2.33%	26.99%	70.68%
None	31.86%	23.69%	43.81%
PE	68.37%	16.85%	14.13%
Lead	53.80%	19.33%	26.23%
Concrete	65.23%	17.72%	16.41%
Water	68.18%	16.69%	14.48%

*This data was not part of the field modifier but included for the purpose of comparison.

Meanwhile, the change in neutron energy distribution or the neutron spectra was also evident for different field modifiers that were incorporated in the computational model. For the same declared dimensions of the modifiers, it was observed that the most thermalized spectrum at the detector location with 68.37% thermal neutrons was obtained by a polyethylene material. The results obtained for the water modifier were comparable, which further confirmed the importance of PE and water as neutron moderators. Concrete, which is the typical material used for accelerator walls, closely followed with 65.23% thermal neutrons, while lead was the least effective in moderating neutrons among the materials investigated (53.80%). Nevertheless, lead is an important component of some accelerator devices and is commonly used for gamma radiation shielding, thus warranting the investigation of neutron interactions with it.

These results are comparable to the reported data from the study of Vega-Carillo *et al*. (2010), who investigated the change in neutron spectra that results from using water and polyethylene as moderators surrounding the neutron source. The neutron spectrum plots in Figure 5 also resemble the data obtained in the study of variation in neutron spectra at different locations in a LINAC radiotherapy facility change (Fontanilla *et al*., 2020).

3.2 Variation in Neutron Field

In addition to investigating the effect of the modifiers on the neutron fluence rate and the neutron spectrum at the detector location, the researchers also analyzed the effect in the neutron field or the spatial distribution of the neutron fluence rate over specified areas of the PNL irradiation room via mesh calculations. The results of mesh calculations, described in section 2, are presented in Figure 6 showing the vertical and horizontal neutron fluence rate distribution with different field modifiers.

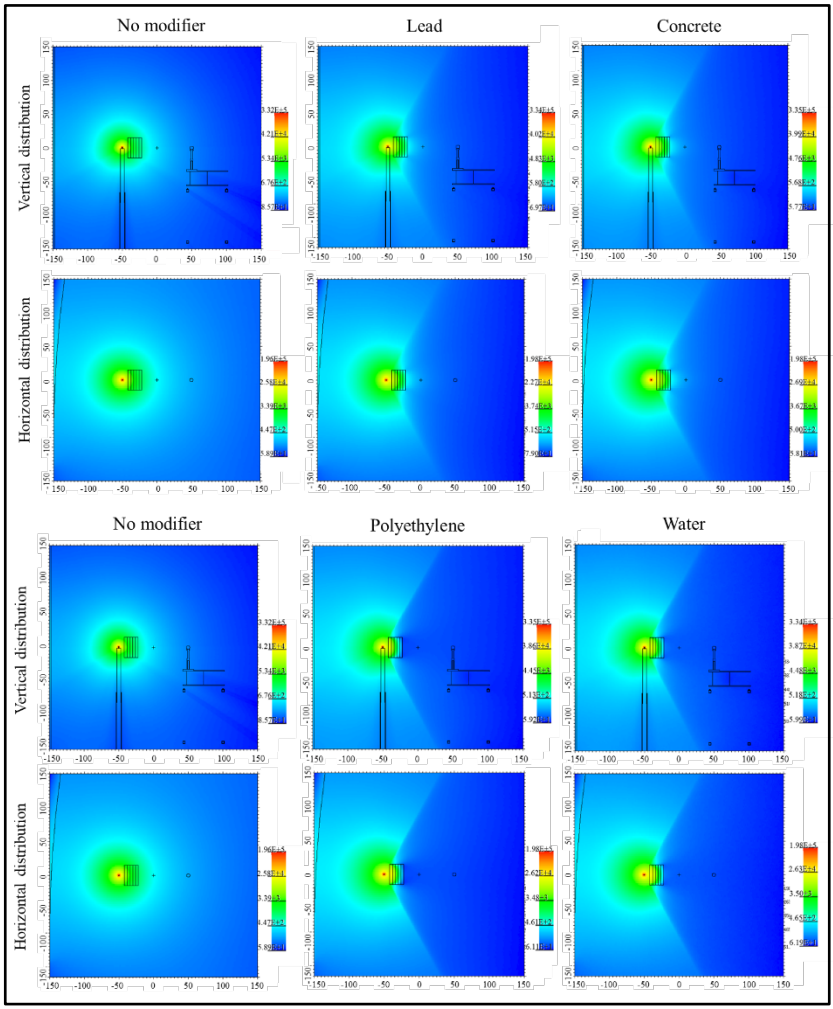

Figure 6. Spatial distribution of total neutron fluence in the 300 x 300 cm area with different modifiers at the PNL irradiation room

It was evident that introducing any of the field modifiers in the computational model resulted in a significant change in the neutron field. The "shadow" cast by the modifier cell in the field demonstrated that a small volume of material lead to a significant change in the field. However, aside from the obvious distortion of the field from the location of the modifier towards the right side of the area considered, there was no easily discernible difference between the fields produced with material modifiers. To investigate the expected modification between these fields, mesh data subtraction was performed.

Figure 7 shows the results of mesh data subtraction between the unmodified field and each of the modified fields. Zero to negative mesh difference values are in color gray to distinguish between positive and negative values.

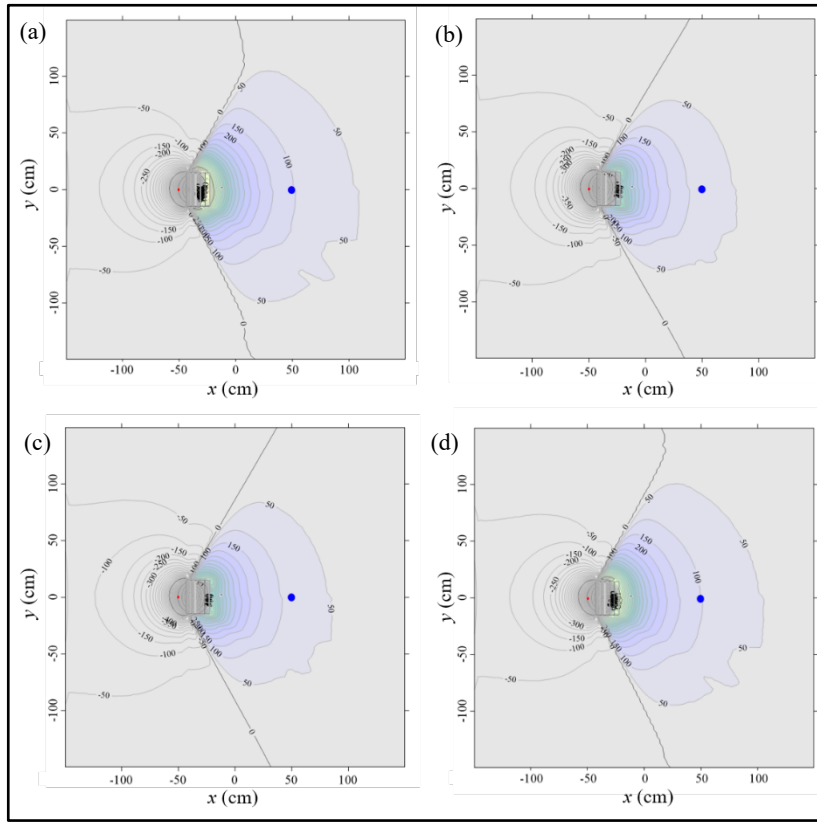

Zero to negative difference values are colored gray. The small red dot indicates the location of the source while the location of the detector is marked by the blue circle.

Figure 7. Horizontal distribution of the neutron fluence rate difference between unmodified and PE-modified (a), lead-modified (b), concrete-modified (c) and water-modified (d) fields

Positive difference values indicated that the presence of the modifier decreased the fluence rate in the region, while areas with negative values showed that the introduction of the modifier resulted in a higher fluence rate in the region, which was a consequence of neutron scattering. A similar trend was observed for all plots with positive difference values at the modifier "shadow" area while zero to negative values were found everywhere else. Nevertheless, results obtained from the mesh subtraction indicated the variations in the fields for different material modifiers used. This was observed from the varying shapes of the contour lines in the plot. It also demonstrated that the modifier affected both the direct neutrons from the source as well as the scattered neutron components.

3.3 Comparison of Ambient Dose Equivalent Rates of Two Modified Spectra

To investigate the effect of field modification on neutron dose, the researchers compared the normalized spectrum obtained from an unmodified field (ϕ_0) and polyethylene-modified field (ϕ_{PE}) against the fluence-to-dose conversion factor (CF) based on International Committee on Radiological Protection (ICRP)-74 (ICRP, 1996) as shown in Figure 8.

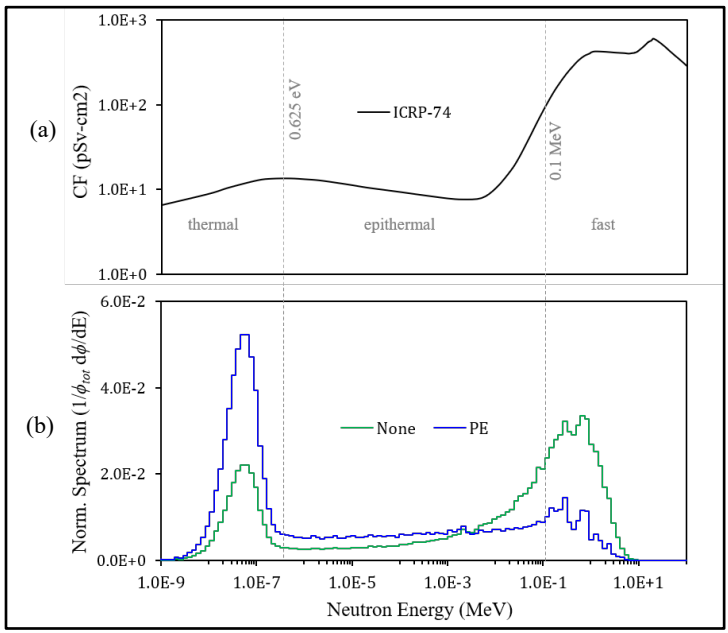

Figure 8. Fluence rate-to-ambient dose conversion factor (CF) based on ICRP-74 (a) and calculated spectra at detector location without modifier and with polyethylene modifier (b)

Since the fast neutron component of ϕ_{PE} was significantly lower than that of ϕ_0, the simple visual comparison showed that the sum-product of the CF with ϕ_{PE} differed from its sum-product with ϕ_0. This demonstrated that since the conversion coefficients were fixed, variations in the neutron spectrum yielded a different value of the ambient dose.

The ambient dose was calculated by getting the sum product of the normalized neutron fluence per energy bin ($d\phi/dE_i$) with the corresponding CF_{Ei} for each energy bin i: $\sum_{i=1}^{120}(d\phi/dE_i)(CF_{Ei})$. The calculated ambient neutron dose rate values relative to the different spectra investigated in this work are presented in Table 4. Neutron spectrum modified with PE and water had the greatest deviation with 96 and 94%, respectively, followed by concrete (83%). The lead-modified spectrum, having the least thermalized neutron components among the modified fields, had the least deviation at 47%.

Table 4. Ambient neutron dose rate per unit fluence corresponding to various neutron spectra

Field modifier	Ambient dose* (μSv/hr)	Relative deviation** (%)
None	7.06E+01	NA
Polyethylene	2.48E+01	96
Lead	4.36E+01	47
Concrete	2.92E+01	83
Water	2.56E+01	94

*Per unit fluence; **with respect to the unmodified field

4. Conclusion and Recommendation

This study was conducted to demonstrate that neutron fields can be modified significantly with the presence of small volume materials found in medical accelerator facilities. Results indicated that field modification was more significant with lighter materials such as polyethylene and water, which considerably reduced fast neutron components due to their high hydrogen content. The highest deviation in ambient dose was for PE-modified spectrum, which was around 96 and 47% for lead-modified spectrum. The result of this work was used as a basis for experiments that were performed at the PNL to investigate the limitations of commercial neutron survey meters when

conducting dose measurements in different neutron fields. Future work will also include modeling of actual materials to be used in experiments.

5. Acknowledgement

This work was supported by the Department of Science and Technology – Philippine Council for Industry, Energy and Emerging Technology Research and Development (DOST-PCIEERD) through the project "Establishment of the PRR-1 Subcritical Assembly for Training, Education, and Research" with Project No. 08669.

6. References

Asuncion-Astronomo, A., Balderas, C.V., Hila, F.C., Dela Cruz, R.M., Dingle, C.A., Solmeron, W.B., & Bedogni, R. (2021). Validation of an indium-based multi-shell neutron spectrometer. Applied Radiation and Isotopes, 170, 109629. https://doi.org/10.1016/j.apradiso.2021.109629

Asuncion-Astronomo, A., Dingle, C.A., Hila, F.C., Balderas, C.V., Silvestre, C.P., Dela Cruz, R.M., & Bedogni, R. (2021). Response matrix validation of a 3He-based multi-shell neutron spectrometer. Nuclear Instruments and Methods in Physics Research Section A: Accelerators, Spectrometers, Detectors and Associated Equipment, 989, 164938. https://doi.org/10.1016/j.nima.2020.164938

Brown, D.A., Chadwick, M.B., Capote, R., Khaler, A.C., Trkov, A., Herman, M.W., Sonzogni, A.A., Danon, Y., Carlson, A.D., Dunn, M., Smith, D.L., Hale, G.M., Arbanas, G., Arcilla, R., Bates, C.R., Beck, B., Becker, B., Brown, F., Casperson, R.J., Conlin, J., …& Zhu, Y. (2018). ENDF/B-VIII.0: The 8th major release of the nuclear reaction data library with CIELO-project cross sections, new standards and thermal scattering data. Nuclear Data Sheets, 148, 1-142. doi:10.1016/j.nds.2018.02.001

Cevallos-Robalino, L.E., García-Fernández, G.F., Lorente, A., Gallego, E., Vega-Carrillo, H.R., & Guzmán-Garcia, K.A. (2019). Design by Monte Carlo method of a thermal neutron device using a $^{241}Am/^{9}Be$ source and high-density polyethylene moderator. Applied Radiation and Isotopes, 151, 150-156. https://doi.org/10.1016/j.apradiso.2019.05.040

Chadwick, M.B., Herman, M., Obložinský, P., Dunn, M.E., Danon, Y., Khaler, A.C., Pritychenko, B., Arbanas, B., Arcilla, R., Brewer, R., Brown, D.A., Capote, R., Carlson, A.D., Cho, Y.S., Derrien, H., Guber, K., Hale, G.M, Hoblit, S., Holloway, S., Johnson, T.D., …& Young, P.G. (2011). ENDF/B-VII.1 nuclear data for science and technology: Cross sections, covariances, fission product yields and decay data. Nuclear Data Sheets, 112(12), 2887-2996. https://doi.org/10.1016/j.nds.2011.11.002

Fontanilla, A.M., Asuncion-Astronomo, A.M., Silvestre, C., Balderas, C., Manlapaz, D.J., & Caballar, R.C. (2020) Evaluation of the neutron spectra in a medical accelerator facility using a modified Bonner sphere spectrometer. Proceedings of the Samahang Pisika ng Pilipinas, 38th International Physics Conference, SPP-2020-2C-05.

Grande, M.L.M.L., Hila, F.C., Garalde, A.A.N.M., Betos, C.M.T., Dingle, C.A.M., & Romallosa, K.M.D. (2020). Experimental, computational, and analytical methods for the characterization of a neutron field for calibration of neutron monitoring instruments in the Philippines. Philippine Journal of Science, (Special Issue), 93-99.

Hila, F.C., Dingle, C.A., Asuncion-Astronomo, A., Balderas, C.V., Grande, M.L., Romallosa, K.M., & Guillermo, N.R. (2021). Evaluation of time-dependent strengths of californium neutron sources by decay of ^{252}Cf, ^{250}Cf, and ^{248}Cm: Uncertainties by Monte Carlo method. Applied Radiation and Isotopes, 167, 109454. https://doi.org/10.1016/j.apradiso.2020.109454

International Committee on Radiological Protection (ICRP). (1996). Conversion coefficients for use in radiological protection against external radiation. In H. Smith (Ed.). Oxford, United Kingdom: Pergamon, Elsevier Science Ltd.

International Organization for Standardization (ISO). (2000). Reference neutron radiations. Part 2: Calibration fundamentals of radiation protection devices related to the basic quantities characterizing the radiation field (ISO 8529-2: 2000). Geneva, Switzerland: ISO.

McConn, R.J., Gesh, C.J., Pagh, R.T., Rucker, R.A., & Williams, R., III. (2011). Compendium of material composition data for radiation transport modeling. Retrieved from https://www.pnnl.gov/main/publications/external/technical_reports/PNNL-15870Rev1.pdf

Qi, P., Wang, Z., Chen, X., Li, X., Chen, Q., Li, Y., Zhao, C., Mao, X., Gao, T., Zhao, Q., Tao, M., Li, F., Zhang, Z., Wu, H., Zhou, R., & Yang, C. (2021). Design and performance of the water-moderator nested spheres neutron spectrometer. Nuclear Instruments and Methods in Physics Research Section A: Accelerators, Spectrometers, Detectors and Associated Equipment, 988, 164868. https://doi.org/10.1016/j.nima.2020.164868

Solmeron, W.B., Asuncion-Astronomo, A., Balderas, C.V., Dela Cruz, R.M.M., & Dela Cruz, J.M. (2020). Neutron spectrometry in a PET cyclotron with a Bonner sphere system. Proceedings of the International Youth Nuclear Congress 2020, Sydney, Australia.

Vega-Carillo, H.R., Ortiz-Rodriguez, J.M., Hernandez-Davila, V.M., Martinez-Blanco, M.R., Hernandez-Almaraz, B., & Ortiz-Hernandez, A.A. (2010) Different spectra with the same neutron source. Revista Mexicana de Física, 56(1), 35-39.